

# An all-silicon linear chain NMR quantum computer

Kohei M. Itoh\*

*Department of Applied Physics and CREST-JST, Keio University, Yokohama 223-8522, Japan*

Received 22 October 2004; accepted 29 October 2004 by the guest editors

Available online 25 January 2005

## Abstract

An updated version of our all-silicon quantum computing scheme [T.D. Ladd, J.R. Goldman, F. Yamaguchi, Y. Yamamoto, E. Abe, K.M. Itoh, Phys. Rev. Lett. 89 (2002) 017901. [3]] and the experimental progress towards its realization are discussed. We emphasize the importance of revisiting a wide range of isotope effects which have been explored over the past several decades for the construction of solid-state silicon quantum computers. Using RF decoupling techniques [T.D. Ladd, D. Maryenko, Y. Yamamoto, E. Abe, K.M. Itoh, Phys. Rev. B. 71 (2005) 014401] phase decoherence times  $T_2 = 25$  s of  $^{29}\text{Si}$  nuclear spins in single-crystal Si have been obtained at room temperature. We show that a linear chain of  $^{29}\text{Si}$  stable isotopes with nuclear spin  $I = 1/2$  embedded in a spin free  $^{28}\text{Si}$  stable isotope matrix can form an ideal building block for solid-state quantum information processors, especially, in the form of a quantum memory which requires a large number of operations within  $T_2$  for the continuous error correction.

© 2005 Elsevier Ltd. All rights reserved.

PACS: 03.67.Lx

Keywords: A. Semiconductors; C. Scanning tunnelling microscopy; D. Spin dynamics

## 1. Introduction

Traditionally, the principal determinants of the properties of a semiconductor are elemental composition and structure, with the elements adequately characterized by their atomic numbers. In recent years, however, isotopic composition has turned out to be another very important determinant of optical, electrical, and magnetic properties of semiconductors [1,2]. By controlling the relative concentrations of the stable isotopes that constitutes the host semiconductors, one can change mass numbers and nuclear spin states of the lattice. For example, in naturally available silicon ( $^{\text{nat}}\text{Si}$ ), which is composed of three stable isotopes at fixed proportions ( $^{28}\text{Si}$  92.2 at.%,  $^{29}\text{Si}$  4.7 at.%, and  $^{30}\text{Si}$  3.1 at.%), the mass difference of  $\sim 7\%$  between  $^{28}\text{Si}$  and

$^{30}\text{Si}$  and/or the nuclear spin difference between the  $I = 1/2$  of  $^{29}\text{Si}$  and the  $I = 0$  of  $^{28}\text{Si}$  and  $^{30}\text{Si}$  can affect significantly some of the properties of silicon. In this paper, we discuss how nuclear spins of  $^{29}\text{Si}$  embedded in a nuclear spin free matrix of  $^{28}\text{Si}$  can be utilized to construct a silicon-based NMR quantum computer [3,4].

The pioneering work on isotope based spin properties was performed by Gordon and Bowers in 1958 [5]. They prepared an isotopically enriched  $^{28}\text{Si}$  single crystal that was depleted of  $^{29}\text{Si}$  with nuclear spins and investigated the spin resonance of electrons bound to phosphorus donors at low temperatures. Such studies were revisited by Tyryshkin et al. more recently to probe the intrinsic electron spin coherence time in silicon without decoherence caused by interaction with host  $^{29}\text{Si}$  nuclear spins [6]. The motivation of Tyryshkin et al. to revisit the isotope effect of electrons bound to phosphorus was to test the feasibility of using phosphorus for construction of a silicon based quantum computer.

\* Tel.: +81 45 566 1594; fax: +81 45 566 1587.

E-mail address: [kitoh@appi.keio.ac.jp](mailto:kitoh@appi.keio.ac.jp).

The first silicon-based quantum computer scheme was put forth by Kane in 1998 [7]. He proposed to use the nuclear spin  $I = 1/2$  of  $^{31}\text{P}$  isotopes embedded in the nuclear spin free matrix of  $^{28}\text{Si}$ . Later, electron spin-based silicon quantum computers, which also require enrichment of Si and Ge isotopes with no nuclear spins, were discussed [8,9]. Our group [3,4] and Shlimak's group [10] proposed independently new silicon-based quantum computer structures utilizing the  $^{29}\text{Si}$  nuclear spins embedded in the spin free matrix of  $^{28}\text{Si}$ . In this work, we will describe an updated version of our all-silicon quantum computer scheme and the progress towards its realization.

## 2. An all-silicon linear chain NMR quantum computer

DiVincenzo stated the following five criteria for the construction of operational quantum computers: [11]

- (i) A scalable physical system with well-defined qubits is preparable.
- (ii) Qubits are initializable to a simple state such as  $|000\dots\rangle$  at the beginning of a calculation.
- (iii) Qubits have adequately long decoherence times.
- (iv) A universal set of quantum gates are performable.
- (v) Each qubit state is measurable with high quantum efficiency.

Fig. 1 shows the overview of our all-silicon linear chain NMR quantum computer. It consists of a linear chain of  $^{29}\text{Si}$  qubits placed on (or in) the substrate of the nuclear spin free  $^{28}\text{Si}$  substrate. A NiFe magnetic stripe is placed at one end of the chain to initialize the spins (Section 2.2) and to apply a large magnetic field gradient for the selective universal gate operation (Section 2.4). A single phosphorus impurity is placed at the opposite end of the chain for initialization (Section 2.2) and read-out (Section 2.5). The whole structure is placed in the 7 T static magnetic field of a NMR spectrometer and is maintained at a stable temperature below 5 K. We shall describe in the following subsections

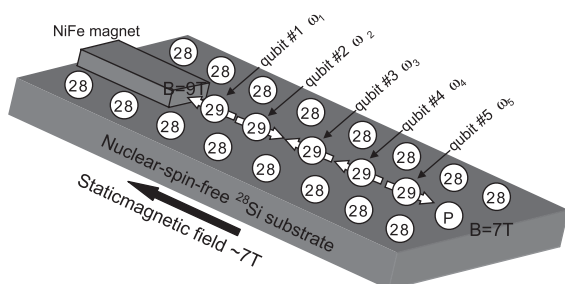


Fig. 1. Five-qubit  $^{29}\text{Si}$  NMR quantum computer with a field gradient applied in the direction of the qubit chain by a NiFe stripe. The entire structure is placed in a conventional NMR spectrometer to perform quantum computing in a very similar way to that which has been conducted in solution NMR quantum computing.

how we may be able to meet DiVincenzo's criteria in our scheme.

### 2.1. Preparation of scalable qubits

A linear chain of  $^{29}\text{Si}$  qubits is prepared on the spin-free matrix of  $^{28}\text{Si}$  substrate in order to meet the criterion (i) of DiVincenzo. Fig. 2(a) shows a schematic of our approach to prepare such a linear chain. At first, a  $^{28}\text{Si}$  substrate with atomically straight step-edges is prepared by appropriate heat treatment of an intentionally off-angled (111) Si wafers using the method developed by Himpfel and co-workers [12]. After such an ideal substrate has been prepared,  $^{29}\text{Si}$  isotopes are deposited in an ultra-high vacuum forming an atomically straight, single  $^{29}\text{Si}$  wire at every step-edge in the step-flow mode of epitaxial growth. We will employ such wires for quantum computation. Fig. 2(b) shows the experimentally obtained scanning tunneling microscope image of a straight step edge structure we have achieved by modifying the annealing sequence of Himpfel and co-workers [13]. To form such  $^{29}\text{Si}$  wires, we used (111) oriented Si wafers with an intentional miscut of  $1^\circ$  towards the  $[\bar{1}\bar{1}2]$  direction and annealed it at  $1260^\circ\text{C}$  for a few seconds for flash cleaning followed by rapid quenching to  $850^\circ\text{C}$  within 3 s. In order to reduce the number of kinks,

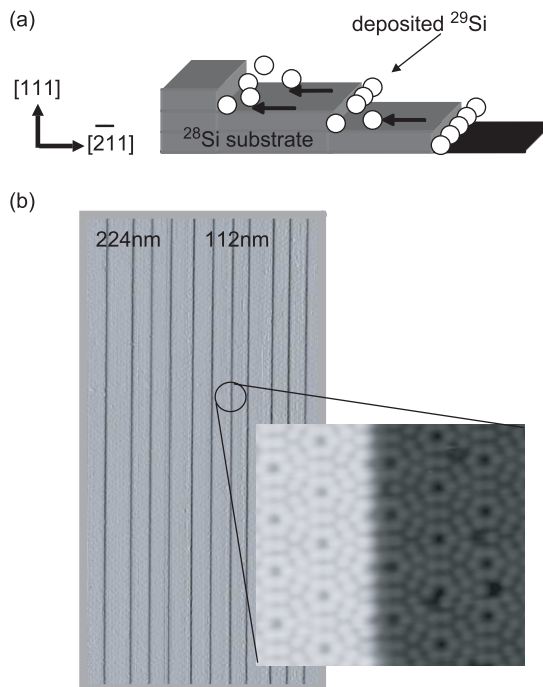


Fig. 2. (a) A schematic of single  $^{29}\text{Si}$  wire formation at the straight step edge of the vicinal  $^{28}\text{Si}$  (111) surface in the step-flow mode of epitaxial growth. (b) A STM picture of the straight step edge vicinal Si (111) surface which has been obtained recently. The right figure is a close up of the step-edge structure showing unique atomic configuration.

we further anneal the sample at 850 °C for ten hours with a DC current flowing along the step-edges. We have determined that the direction of the current must be towards the kinks rather than away from the kinks in order to obtain the straight step-edge structures shown in Fig. 2(b). The STM image in Fig. 2(b) shows kink-less straight step-edges more than 7000 atoms long in the direction of  $[11\bar{2}]$ . Evaporating a small amount of Si on the substrate shown in Fig. 2(b), we have obtained recently a single and straight silicon wire attached to the step-edges [14]. In parallel we have developed the technology to grow and characterize bulk [15] and low-dimensional single crystal silicon [16] with controlled isotopic composition. We are ready to grow atomic wire  $^{29}\text{Si}$  qubits on a  $^{28}\text{Si}$  substrate as shown in Fig. 1.

Fig. 3 shows the NiFe magnetic stripes we have developed recently for electron spin injection for initialization (Section 2.2) and for selective manipulation of each  $^{29}\text{Si}$  qubit (Section 2.4) [17]. In order to prepare these magnetic stripes, a 200 nm thick Ti, a 1  $\mu\text{m}$  thick  $\text{Ni}_{45}\text{Fe}_{55}$  thin film, and a 8 nm thick Ti layer of were deposited by ion beam sputtering. The top Ti layer served as a mask material for etching the  $\text{Ni}_{45}\text{Fe}_{55}$  thin film, while the Ti interlayer was used to improve the bonding strength between the Si (001) and the  $\text{Ni}_{45}\text{Fe}_{55}$  thin film. The Ti was patterned by photolithography with a UV cure and dry-etched by reactive ion etching (RIE) using  $\text{SF}_6$  gas. The patterned Ti mask was then used to etch the  $\text{Ni}_{45}\text{Fe}_{55}$  thin film in the same chamber using RIE in a gas mixture of CO,  $\text{NH}_3$  and Xe [17].

It is now possible to prepare the structure shown in Fig. 1, namely a scalable  $^{29}\text{Si}$  qubit wire with a magnet for initialization and a large magnetic field gradient for selective qubit manipulation.

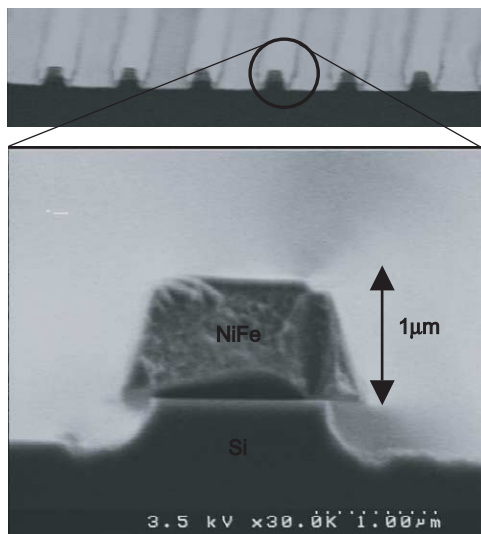


Fig. 3. An array of ferromagnetic strips formed on Si (above) and the cross section of one stripe (below).

## 2.2. Initialization

Because we place the structure shown in Fig. 1 in the static magnetic field of 7 T, one may think that it is possible to orient most of the  $^{29}\text{Si}$  nuclear spins in one direction (namely in the  $|000\dots\rangle$  state) simply by cooling the structure below the energy of the nuclear spin Zeeman splitting. However, the small magnetic moment of nuclear spins requires cooling down to  $\mu\text{K}$  (micro Kelvin), which, of course, is unrealistic. To overcome this impediment, we are pursuing the following three alternatives. The first one is the injection of spin polarized electrons from the NiFe stripe into the Si bulk in order to induce spin flip–flops between injected electron spins and  $^{29}\text{Si}$  nuclear spin qubits. The second option involves shining intense, above bandgap light on the structure. We have recently used 1024.8 nm wavelength light corresponding to photon energy of 1.21 eV to excite electron–hole pairs in a NMR spectrometer and found a nuclear polarization increase up to  $\sim 0.25\%$  which is about three orders of magnitudes larger than the thermal equilibrium polarization [18]. We have modeled such a process with nuclear spin polarization mediated by electron–hole pair excitation and plan to increase the current level of 0.25% to much larger polarization values [18]. The third option is to inject spin polarized electrons from the decay of donor bound excitons. It has been shown that phosphorus bound exciton transition lines in isotopically enriched  $^{28}\text{Si}$  are much narrower than those in  $^{nat}\text{Si}$  [19], allowing for the selective excitation of a specific donor bound exciton state with appropriate electron and hole polarizations with a well-defined laser energy. When such an exciton decays, a free electron and a hole with specific spin states are injected into the region where  $^{29}\text{Si}$  qubits are situated and this will orient the nuclear spins via flip–flop processes.

## 2.3. $^{29}\text{Si}$ nuclear spin coherence time

Quantum calculations require an ability to couple and decouple interactions between qubits. For example, those qubits that are subject to single qubit operations (e.g. control of amplitude or phase of selected individual spins) must be completely decoupled from other qubits and environment such that unwanted interactions will not to interfere with the precise operation of the single qubit gates. Two-qubit operations similarly require decoupling of the two qubits completely from other qubits and the environment while maximizing the coupling between the two qubits. Therefore, the ability to couple and decouple qubits freely is a major prerequisite for the realization of operational quantum computers.

The major source of decoherence of  $^{29}\text{Si}$  nuclear spins in high quality silicon single crystals was confirmed to be dipolar couplings between  $^{29}\text{Si}$  nuclear spins [20]. The dipolar coupling in a rotating reference frame is written as

$$H = \sum_{j \neq k} D_{jk} [\mathbf{I}_j \cdot \mathbf{I}_k - 3I_j^z I_k^z] \quad (1)$$

where

$$D_{ik} = \hbar^2 \gamma^2 \frac{1 - 3 \cos^2 \theta_{jk}}{r_{jk}^3} \quad (2)$$

Here  $\mathbf{I}_j$  and  $\mathbf{I}_k$  are the spin operators for the  $j$ th and  $k$ th spins, respectively.  $D_{jk}$  (the coupling constant between  $j$ th and  $k$ th spin) is not constant, due to the random distribution of  $^{29}\text{Si}$  in the bulk crystals.  $T_2$  of  $^{29}\text{Si}$  nuclear spins in  $^{\text{nat}}\text{Si}$  that contains 4.7% of  $^{29}\text{Si}$  at room temperature without decoupling of dipolar interactions was found to be 200 ms [21]. In order to extend this  $T_2$ , we have recently applied appropriate high-power RF decoupling pulse sequences and succeeded in extending  $T_2$  to as much as 25 s [22]. The decoupling pulse sequences we have employed is referred to as the MREV-16 among NMR spectroscopists, which is an extended version of the well-known MREV-8 [23]. Such pulse sequences rotate spins cyclically, with the interval being much faster than  $T_2$ , and perform inverse spin operations against time evolution of the Hamiltonian due to the dipolar term of Eq. (2).  $T_2 \sim 25$  s is by far the longest  $T_2$  obtained experimentally for solid-state qubits as seen in

Table 1. We have also studied  $T_2$  as a function of the  $^{29}\text{Si}$  concentration and of  $1/f$  noise due arising from charge fluctuation of unidentified defects, which is another important source of decoherence along with nuclear dipole interactions. Details are described in Ref. [22].

#### 2.4. Spin manipulation

Nuclear spin manipulation using RF pulses is well-established. For example, the decoupling pulse sequence we have applied successfully to switch off unwanted interactions represents one of important spin manipulation processes. As shown in Fig. 1, each  $^{29}\text{Si}$  is a qubit and its NMR frequency is separated from others by a strong magnetic field gradient in the direction of the chain due to the completely magnetized ferromagnetic stripes (NiFe). Therefore, one can manipulate spins selectively with NMR frequencies specific to the target spins. Table 1 compares  $QT_2$  and  $JT_2$  that are the estimated maximum numbers of single- and two-qubit operations, respectively, performable within  $T_2$ . Clearly,  $^{29}\text{Si}$  nuclear spin qubits outperform other qubits in  $QT_2$  and  $JT_2$ , supporting high expectations for the feasibility of all-silicon quantum computer.

Table 1

A list of experimentally obtained coherence times  $T_2$  for various qubits compiled by T.D. Ladd of Stanford University

Qubit	$\omega_0/2\pi$	$T_2$	$Q$	$QT_2$	$JT_2$	Reference
Trapped optical ions ( $^{40}\text{Ca}^+$ )	412 THz	1 ms	$10^{12}$	$10^2$	$10^1$ – $10^3$	[24]
Trapped micro-wave ions ( $^9\text{Be}^+$ )	1.25 GHz	1 ms	$10^6$	$10^3$	$10^1$ – $10^3$	[25]
Molecular nuclei in liquid solution	500 MHz	2 s	$10^9$	$10^5$	$10^2$	[26]
Charge states in quantum dots	200–600 THz	40–630 ps	$10^5$	$10^2$	$10^2$	[27]
Josephson–junction flux qubits	6.6 GHz	30 ns	$10^3$	$10^2$	$10^1$	[28]
Josephson–junction charge qubits	16 GHz	500 ns	$10^4$	$10^2$	$10^4$	[29]
Josephson–junction phase qubits	16 GHz	5 $\mu\text{s}$	$10^5$	$10^1$	$10^4$	[30]
Electron spins bound to donors in Si	10 GHz	3 ms	$10^7$	$10^5$	–	[6]
N–V centers in diamond	120 MHz	1 ms	$10^5$	$10^5$	$10^3$	[31]
$^{29}\text{Si}$ nuclei in solid silicon	60 MHz	25 s	$10^9$	$10^6$	$10^4$	[21]

Most of these times were measured by spin-echo Ramsey spectroscopy or four-wave-mixing.  $Q$  is the product of the fundamental qubit frequency  $\omega_0/2\pi$  and  $\pi T_2$ . The  $QT_2$  column shows the experimental product of the Rabi frequency and the coherence time; this provides a more realistic measure than  $Q$  of the available number of sequential single-qubit gates. Technical improvements can increase  $QT_2$  as far as  $Q$  in some architectures, while for others  $Q$  must be limited in order to maintain selective qubit control. The  $JT_2$  column shows the product of the coherence time and the measured or expected qubit–qubit coupling speed; roughly the available number of sequential two-qubit gates.

### 2.5. Spin read-out

At the end of a quantum computation, one has to read out the quantum states of the qubits. Because the magnetic moment of a single nuclear spin is too small for a one-qubit detection using today's technology, we are investigating a method to detect single nuclear spin states indirectly via photoluminescence [32] or electron paramagnetic spin resonance (EPR) [33] of phosphorus impurities in Si. For the EPR detection, we have investigated the effect of host  $^{29}\text{Si}$  on the electron spin coherence of phosphorus bound electrons using a phosphorus-doped isotopically enriched  $^{29}\text{Si}$  bulk single crystal enriched to 99.23% [33]. The host  $^{29}\text{Si}$  nuclear spins cause local fluctuation of the magnetic field due to the mutual flip-flops, leading to electron spin decoherence. Moreover, hyperfine interactions between the electron spin and the host nuclear spins were probed with the electron-spin-echo-envelope-modulation (ESEEM) effect. If the hyperfine interaction is mostly anisotropic, and its amplitude is comparable to the nuclear Zeeman interaction, a formally forbidden nuclear-spin-flip transition is allowed due to the state mixing, and the ESEEM arises from interference between the allowed and forbidden transitions induced by the strong microwave pulses. Frequency-domain analysis revealed that the ESEEM originates mainly from the interactions between the electron and nearest neighbor  $^{29}\text{Si}$  nuclei to phosphorus and therefore, single nuclear spin detection may be possible through EPR of donor bound single electrons [33].

### 3. Summary

We have discussed the updated version of a solid-state silicon NMR quantum computer architecture that meets the five criteria of DiVincenzo for construction of operational quantum computers. The decoherence time  $T_2$  of the  $^{29}\text{Si}$  qubits in Si single crystals has been extended up 25 s at room temperature by irradiation with dipolar decoupling pulse sequences. Within  $T_2 \sim 25$  s, it is possible to perform  $10^6$  single qubit and  $10^4$  two-qubit operations, which are the largest number of performable gates in the solid-state systems. Recent advances in quantum error-correcting codes and fault tolerant quantum computation schemes implies that it is possible to perform large-scale quantum computation even in the presence of decoherence if more than  $10^6$  single- and two-qubit gates are performable within the coherence time  $T_2$ . We plan to extend our  $T_2$  by two orders of magnitudes in order to allow for practical fault-tolerant quantum computing with solid silicon.

### Acknowledgements

This work has been conducted in collaboration with Y. Yamamoto, T.D. Ladd, J.R. Goldman, Y. Ohno, S. Sasaki,

Y. Matsumoto, M. Esashi, D. Wang, T. Sekiguchi, S. Yoshida, E. Abe, A. Takahashi, and R. Van Meter. We extend our sincere thanks to E.E. Haller for fruitful discussions. The work was supported partly by a Grant-in-Aid for Scientific Research in Priority Areas 'Semiconductor-Nanospintronics' from the Ministry of Education, Culture, Sports, Science, and Technology, Japan.

### References

- [1] E.E. Haller, *J. Appl. Phys.* 77 (1995) 2857.
- [2] F. Widulle, T. Ruf, M. Konuma, I. Silier, M. Cardona, W. Kriegseis, V.I. Ozhogin, *Solid State Commun.* 118 (2001) 1.
- [3] T.D. Ladd, J.R. Goldman, F. Yamaguchi, Y. Yamamoto, E. Abe, K.M. Itoh, *Phys. Rev. Lett.* 89 (2002) 017901.
- [4] E. Abe, K.M. Itoh, T.D. Ladd, J.R. Goldman, F. Yamaguchi, Y. Yamamoto, *J. Supercond.* 16 (2003) 175.
- [5] J.P. Gordon, K.D. Bowers, *Phys. Rev. Lett.* 1 (1958) 368.
- [6] A.M. Tyryshkin, S.A. Lyon, A.V. Astashkin, A.M. Raitsimring, *Phys. Rev. B* 68 (2003) 193207.
- [7] B.E. Kane, *Nature* 393 (1998) 133.
- [8] R. Vrijen, E. Yablonovitch, K. Wang, H.W. Jiang, A. Balandin, V. Roychowdhury, T. Mor, D. DiVincenzo, *Phys. Rev. A* 62 (2000) 012306.
- [9] G.P. Berman, G.D. Doolen, P.C. Hammel, V.I. Tsifrinovich, *Phys. Rev. Lett.* 86 (2001) 2894.
- [10] I. Shlimak I, V.I. Safarov, I.D. Vagner, *J. Phys.: Condens. Matter* 13 (2001) 6059.
- [11] D.P. DiVincenzo, *Science* 270 (1995) 255.
- [12] J.-L. Lin, D.Y. Petrovykh, J. Viernow, F.K. Men, D.J. Seo, F.J. Himpsel, *J. Appl. Phys.* 84 (1998) 255.
- [13] S. Yoshida, T. Sekiguchi, K.M. Itoh, unpublished.
- [14] T. Sekiguchi, S. Yoshida, K.M. Itoh, submitted for publication.
- [15] K.M. Itoh, J. Kato, F. Uemura, A.K. Kaliteyevskii, O.N. Godisov, G.G. Devyatych, A.D. Bulanov, A.V. Gusev, I.D. Kovalev, P.G. Sennikov, H.-J. Pohl, N.V. Abrosimov, H. Riemann, *Jpn. J. Appl. Phys.* 42 (Pt. 1) (2003) 6248.
- [16] T. Kojima, R. Nebashi, K.M. Itoh, Y. Shiraki, *Appl. Phys. Lett.* 83 (2003) 2318.
- [17] D.F. Wang, T. Ono, A. Takahashi, Y. Matsumoto, K.M. Itoh, Y. Yamamoto, M. Esashi, *Proceedings of the 18th European Conference on Solid-State Transducers (Euroensors XVIII)*, 2004, p. 586–589.
- [18] A.S. Verhulst, Y. Yamamoto, K.M. Itoh, *Phys. Rev. B* submitted for publication.
- [19] D. Karaiskaj, M.L.W. Thewalt, T. Ruf, M. Cardona, H.-J. Pohl, G.G. Devyatych, P.G. Sennikov, H. Riemann, *Phys. Rev. Lett.* 86 (2001) 6010.
- [20] A.S. Verhulst, D. Maryenko, Y. Yamamoto, K.M. Itoh, *Phys. Rev. B* 68 (2003) 054105.
- [21] S. Watanabe, S. Sasaki, *Jpn. J. Appl. Phys.* 42 (Pt. 1) (2003) L1350.
- [22] T.D. Ladd, D. Maryenko, Y. Yamamoto, E. Abe, and K.M. Itoh, *Phys. Rev. B* 71 (2005) 014401.
- [23] (a) P. Mansfield, M.J. Orchard, D.C. Stalker, K.H. Richards, *Phys. Rev. B* 7 (1973) 90;  
(b) W.K. Rhim, D.D. Elleman, R.W. Vaughan, *J. Chem. Phys.* 59 (1973) 3470.

- [24] (a) F. Schmidt-Kaler, et al., *Nature* 422 (2003) 408;  
(b) F. Schmidt-Kaler, et al., *J. Phys. B* 36 (2003) 623.
- [25] D. Liebfried, et al., *Nature* 422 (2003) 412.
- [26] L.M.K. Vandersypen, et al., *Nature* 414 (2001) 883.
- [27] (a) N.H. Bonadeo, et al., *Science* 282 (1998) 1473;  
(b) M. Bayer, et al., *Science* 291 (2001) 451;  
(c) X. Li, et al., *Science* 301 (2003) 809;  
(d) P. Palinginis, et al., *Phys. Rev. B* 67 (2003) 201307.
- [28] (a) J.E. Mooij, *Science* 285 (1999) 1036;  
(b) I. Chiorescu, et al., *Science* 299 (2003) 1869.
- [29] (a) Y. Makhlin, G. Schön, A. Shnirman, *Nature* 398 (1999) 305;  
(b) Yu.A. Pashkin, et al., *Nature* 421 (2003) 823;  
(c) D. Vion, et al., *Science* 296 (2002) 886.
- [30] (a) Y. Yu, et al., *Science* 296 (2002) 889;  
(b) A.J. Berkley, et al., *Science* 300 (2003) 1548.
- [31] J. Wrachtrup, et al., *Opt. Spectrosc.* 91 (2001) 429.
- [32] K.C. Fu, T.D. Ladd, C. Santori, Y. Yamamoto, *Phys. Rev. B* 69 (2004) 125306.
- [33] E. Abe, K.M. Itoh, J. Isoya, S. Yamasaki, *Phys. Rev. B* 70 (2004) 033204.